TECHNICAL NOTES

NATIONAL ADVISORY COMMITTEE FOR AERONAUTICS

No. 761

PRESSURE-DISTRIBUTION INVESTIGATION OF AN N.A.C.A. 0009 AIRFOIL WITH AN 80-PERCENT-CHORD PLAIN FLAP AND THREE TABS

By Milton B. Ames, Jr., and Richard I. Sears
Langley Memorial Aeronautical Laboratory

Washington
May 1940

NATIONAL ADVISORY COMMITTEE FOR AERONAUTICS

TECHNICAL NOTE NO. 761

PRESSURE-DISTRIBUTION INVESTIGATION OF AN N.A.C.A. 0009 AIRFOIL WITH AN 80-PERCENT-CHORD PLAIN FLAP AND THREE TABS

By Milton B. Ames, Jr., and Richard I. Sears

SUMMARY

Pressure-distribution tests of an N.A.C.A. 0009 airfoil with an 80-percent-chord plain flap and three plain tabs, having chords of 10, 20, and 30 percent of the flap chord, were made in the N.A.C.A. 4- by 6-foot vertical tunnel. Section data suitable for application to the design of horizontal and vertical tail surfaces were obtained.

Resultant-pressure diagrams for the airfoil with the flap and the 20-percent-chord tab are presented. Plots are also given of increments of normal-force and hinge-moment coefficients for the airfoil, the flap, and the three tabs. A comparison of some characteristic slopes for the 30-, the 50-, and the 80-percent-chord flaps, tested in the general investigation of plain flaps for control surfaces, is included. Section aerodynamic and load data have been made available for a wide range of flap and tab chords to be used on an N.A.C.A. 0009 airfoil or on other conventional sections.

INTRODUCTION

The National Advisory Committee for Aeronautics has conducted investigations of plain flaps and trailing-edge tabs on airfoils of different profiles and with finite spans. The results of some of these investigations are reported in references 1, 2, and 3. No available data applicable to tail-surface design give the aerodynamic section characteristics of a thin airfoil as affected by flaps and tabs of different sizes. In order to provide this information, an investigation was started of an N.A.C.A. 0009 airfoil having flaps and tabs of various chords. The results of the tests of a 50-percent-chord

flap and three tabs are reported in reference 4 and of a 30-percent-chord flap with three tabs, in reference 5. The present report gives the results of pressure-distribution tests on the N.A.C.A. 0009 airfoil with an 80-percent-chord plain flap and three tabs having chords 10, 20, and 30 percent of the flap chord. From the data obtained, normal-force and pitching-moment coefficients were calculated for the airfoil section complete with the flap and the various tabs. In addition, normal-force and hinge-moment coefficients were calculated for the flap with the different tabs and for the tabs alone.

APPARATUS

The tests were conducted in the N.A.C.A. 4- by 6-foot vertical wind tunnel (reference 6) with modifications as shown in figure 1 and described in reference 5. The 3- by 4-foot model was made of mahogany, shaped to the N.A.C.A. 0009 profile. It was equipped with a plain flap having a chord 80 percent of the airfoil chord and three serially hinged plain tabs having chords 10, 20, and 30 percent of the flap chord, as shown in figure 2. The nose radii of the flap and the tabs were approximately one-half the airfoil thickness at the hinge axes. All gaps at the flap and the tab hinges were sealed with plasticine and cellulose tape to prevent air leakage during the tests. A single row of pressure orifices was located at the airfoil midspan, as shown in figure 3.

Because the model completely spanned the test section, two-dimensional flow was approximated. The airfoil was attached to the balance frame by torque tubes, which were extended through the sides of the tunnel and were rotated by a calibrated electric drive outside the tunnel in order to set the angle of attack. Flap and tab deflections were set by varying the position of lever arms on the model. The pressure orifices were connected by rubber tubing to a photographically recording multiple-tube manometer located outside the tunnel.

TESTS

The tests were made at an effective Reynolds Number of 3,410,000. (Effective Reynolds Number = tunnel Reynolds

Number × turbulence factor. The turbulence factor for the 4- by 6-foot vertical tunnel is 1.93.) The average dynamic pressure was 10.8 pounds per square foot, corresponding to an air speed of about 65 miles per hour at standard sea-level conditions. The range of angles of attack from -14-1/2° to 10-1/2° was investigated at intervals of 5°. At each angle of attack, the airfoil was tested with the flap deflected 0°, 5°, 10°, 20°, and 30° down. Tests were made throughout the entire angle-of-attack range for each flap deflection with tab deflections of 0°, ±10°, ±20°, and ±30° for each of the tab sizes.

RESULTS

Presentation of Data

The results of the distribution of pressures are given in the form of resultant-pressure and resultant-pressure-increment diagrams, which represent changes in resultant-pressure distribution caused by a change in angle of any one part or any combination of the component parts of the airfoil. The resultant normal pressure at any point along the chord lines of the airfoil was determined by taking the algebraic difference of the pressures normal to the surfaces of the airfoil at that point. All diagrams of resultant pressure or resultant-pressure increments of the airfoil, flap, and tab combination are plotted as pressure coefficients P or as ΔP, where

$$P = \frac{p - p_o}{q}$$

and

p static pressure at a point on the airfoil.

p_o static pressure in free air stream.

q dynamic pressure of free air stream.

Resultant-pressure diagrams are given in figure 4 for the basic section (i.e., with flap and tab neutral). The resultant-pressure diagram for any other condition may be obtained by adding (to the basic diagram) the resultant-pressure increment for the particular condition. The resultant-pressure-increment diagrams are given in figures 5 to 9.

Because the large quantity of data prohibited the inclusion of all the resultant-pressure-increment diagrams for all tab sizes, only the diagrams for tab deflections of 0° and $\pm 30^\circ$ for the $0.20c_f$ tab, which was considered to be an average size, are presented. Values of angle of attack were selected to represent (1) an unstalled negative angle of attack, $\alpha = -9\text{-}1/2^\circ$; (2) a low angle of attack, $\alpha = 1/2^\circ$; and (3) an unstalled high angle of attack, $\alpha = 5\text{-}1/2^\circ$. These values of angle of attack were also selected to make the data in this report comparable with the results presented in references 4 and 5.

Previous tests have indicated that the increments of pressure distribution and the increments of section aerodynamic coefficients due to flap deflection are independent of the basic section; it is therefore believed that, for structural-design purposes, the data herein presented may be applied to other basic sections of conventional shape and the same thickness.

The section characteristics of the airfoil, the flap, and the tab, as functions of flap and tab deflection, are also plotted as increments, which were obtained by deducting the basic section coefficients from those for the section with the tab, the flap, or the combination deflected. The characteristics were obtained in each case by mechanical integration of the original plotted pressure diagrams.

Computations were made to determine the section coefficients, which are defined as follows:

$c_n = \frac{n}{qc}$ airfoil section normal-force coefficient.

$c_{m_{c/5}} = \frac{m}{qc^2}$ airfoil section pitching-moment coefficient about the one-fifth-chord point (0.20c point) of the airfoil.

$c_{n_f} = \frac{n_f}{qc_f}$ flap section normal-force coefficient.

$c_{h_f} = \frac{h_f}{qc_f{}^2}$ flap section hinge-moment coefficient.

$c_{n_t} = \frac{n_t}{qc_t}$ tab section normal-force coefficient.

$c_{h_t} = \frac{h_t}{qc_t{}^2}$ tab section hinge-moment coefficient.

where the forces and moments per unit span are:

n normal force of airfoil section.

m pitching moment of airfoil section about the one-fifth-chord point of the airfoil.

n_f normal force of flap section.

h_f hinge moment of flap section.

n_t normal force of tab section.

h_t hinge moment of tab section.

and c chord of basic airfoil with flap and tab neutral.

c_f flap chord.

c_t tab chord.

α angle of attack.

δ deflection of flap or tab.

The subscript f refers to the flap with the tab; and the subscript t, to the tab alone.

The integrated coefficients for the basic airfoil are plotted against angle of attack in figure 10. The increments for various tab and flap deflections are presented in figures 11 to 19.

Precision

As mentioned in reference 5, no air-flow-alinement tests have been made in this tunnel but all angles of attack have been corrected for a misalinement of 1/2° that appeared to be present in the air flow. The absolute flap and tab deflections were correct to within ±2°. The relative angles of attack, however, were set to within ±0.1°, and the relative flap and tab deflections to within ±1.0°. Over most of the airfoil, plotted pressures were accurate to within ±2 percent but, at the peaks, the accuracy was less at high angles of attack. The dynamic-pressure readings were correct to within ±1 percent.

Inasmuch as two-dimensional flow was approximated,

the integrated results may be considered as section characteristics. Corrections for tunnel-wall interference effects were made only to the values of airfoil normal-force coefficient c_n. The corrections for flap and tab coefficients are not definitely known, but the uncorrected values are probably conservative for purposes of stress analysis.

DISCUSSION

Pressure Distribution

The effects of the $0.20c_f$ tab and the 0.80c flap deflections on the distribution of resultant-pressure increments over the main airfoil are shown in figure 4 to 9. These diagrams should be useful for application to the structural design of horizontal and vertical tail surfaces having plain flaps and tabs with very small or sealed gaps. As the same basic section was used in these tests as was used in the tests reported in references 4 and 5, the basic distribution (fig. 4) is the same as was previously obtained.

Because the distribution curves in figures 4 to 9 were plotted from data uncorrected for tunnel effects, the distributions represented in these curves will be high or conservative when used for structural purposes. It likewise should be remembered that sealed gaps were used and consequently high peak pressures were obtained at the flap and the tab hinge axes.

The incremental distributions resulting from the deflection of the $0.20c_f$ tab (fig. 5) show that the highest peak pressures occur at the tab hinge axis. Similarly, when the flap is deflected (figs. 6 to 9), the peak values of the pressure increments on the flap occur at the flap hinge axis.

When the tab and the flap are simultaneously deflected in the same direction, the peak values of the load increments occur at both hinge axes, and the resultant pressures act in the same direction. If the tab and the flap are deflected at the same time in opposite directions, the peak values of the pressure increments occur at both hinge axes but the resultant pressures act in opposite directions (figs. 6 to 9).

Comparison with the resultant-pressure-increment diagrams in references 4 and 5 shows that the shapes of the curves in the different investigations are similar although the greatest loads were, of course, obtained with the largest flap. As shown in reference 5, certain irregularities occurred in the curves over the first 3 percent of the chord from the airfoil nose. These irregular humps may be caused by laminar separation resulting from severe adverse pressure gradients.

Aerodynamic Section Characteristics

Airfoil characteristics.- The basic airfoil section gave results (fig. 10) that are in agreement with the data for the basic sections in references 4 and 5. The slope of the normal-force curve $\partial c_n/\partial\alpha$ is 0.095, which agrees with the slopes obtained in references 4, 5, and 7. A slight discrepancy is noticeable in the data plotted in figure 10, in that the c_n and the $c_{m_{c/5}}$ curves for the airfoil do not pass through zero at 0° angle of attack. This shift of the curves was probably caused by model imperfections and tab misalinement. The airfoil section increment coefficients of normal force and pitching moment are plotted in figures 11, 14, and 17. The maximum value of Δc_n was 2.40 at $\alpha = -14\text{-}1/2°$ with both the flap and the $0.30c_f$ tab deflected 30° (fig. 17(a)). Deflecting the tab to -30° resulted in a value of Δc_n of 1.16. The change in Δc_n with the tab reversed was 1.24, or about 52 percent of the increment with both the flap and the tab deflected in the same direction. Comparisons with references 4 and 5 of changes in the maximum values of Δc_n caused by reversing the tab deflection showed that, for the 0.50c flap, the difference was 42 percent and, for the 0.30c flap, 39 percent.

The stall of the flap, as shown by the data, generally occured at a deflection of about 20° for low angles of attack and at about 5° for the high angles of attack. These points are indicated by the breaks, or change in slope, of the c_n and the $c_{m_{c/5}}$ curves. No test were made of the $0.30c_f$ tab deflected 30° with $\alpha = 10\text{-}1/2°$ because of the stalled and very unsteady flow over the model.

The pitching-moment coefficients of the airfoil are

given about the 0.20c point because it was the location of the flap hinge axis. The results for the basic airfoil section (fig. 10) gave a linear variation of $\Delta c_{m_{c/5}}$ with angle of attack. The values of $\Delta c_{m_{c/5}}$ also varied linearly with δ_f within the unstalled flap range. The effectiveness of the tabs in reducing $\Delta c_{m_{c/5}}$ decreased as the tab deflection was increased positively or negatively from zero.

Flap and tab characteristics.- The flap section increment coefficients, Δc_{n_f} and Δc_{h_f}, varied nearly linearly with flap deflection throughout the unstalled range. It was noted that the 0.80c flap was rather effective, in that small deflections produced large changes in the flap section coefficient increments. In general, the tab deflections shifted Δc_{n_f} and Δc_{h_f} parallel to themselves, and the rate of change of the increments with the tab deflection decreased as the tab deflections increased positively or negatively from the neutral position. The $0.10c_f$ tab deflected -30° was ineffective in reducing Δc_{h_f}. This characteristic is in agreement with the results reported in references 1, 2, and 5. As stated in the discussion of the airfoil characteristics, the flap stalled at a deflection of about 20° for low angles of attack and between 5° and 10° for high angles of attack. At the low angles of attack, the upward deflections of the tabs showed a tendency to delay the flap stall at flap deflections of 20° or 30°.

The increments of tab section normal-force and hinge-moment coefficients tended to vary linearly with tab deflection until the tab stalled. (See figs. 13, 16, and 19.) Deflection of the flap caused greater increments of Δc_{n_f} and Δc_{h_f} when the tab was deflected in the same direction as the flap than when the tab was deflected in the opposite direction. As observed in references 4 and 5, the -30° deflection of the $0.10c_f$ and the $0.20c_f$ tabs frequently gave unsteady or irregular increment coefficients.

Comparison of the Three Sizes of Plain Flap

As a comparison of the general characteristics and as a summary, some average slopes obtained from the ex-

perimentally determined section characteristics of the N.A.C.A. 0009 airfoil with the 0.30c, the 0.50c, and the 0.80c flaps having tabs are given in the following table. (All slopes are for infinite aspect ratio.)

N.A.C.A. 0009 AIRFOIL WITH THREE SIZES OF FLAP AND 0.20c_f TAB

Flap size	$\frac{\partial c_n}{\partial \alpha}$	$\frac{\partial \alpha}{\partial \delta_f}$	$\left(\frac{\partial \delta_f}{\partial \alpha}\right)_{c_h = 0}$	$\frac{\partial c_{hf}}{\partial \delta_f}$	$\frac{\partial c_{hf}}{\partial \delta_t}$	$\frac{\partial \alpha}{\partial \delta_t}$
[a]0.30c	0.095	0.57	-0.52	-0.014	-0.013	0.21
[b].50c	.095	.77	-.76	-.016	-.016	.29
.80c	.095	.96	-.94	-.020	-.019	.39

[a]Data from reference 5.

[b]Data from reference 4.

CONCLUDING REMARKS

With the presentation of data on an 80-percent-chord flap, the investigation of section aerodynamic and load characteristics of an N.A.C.A. 0009 airfoil with a wide range of sizes of flaps and tabs is completed. The data supplied should be applicable to the design of any plain flap and tab combination that is likely to be used for horizontal or vertical tail surfaces. The incremental data presented are believed to be applicable to other conventional airfoils of approximately the same shape and thickness.

In the application of the data, it must be remembered that the results herein contained are for hinged surfaces with completely sealed gaps and that only the values of airfoil normal-force coefficient are corrected for tunnel effects. Although the other coefficients are uncorrected, they are believed to be conservative for application in stress analysis.

Langley Memorial Aeronautical Laboratory,
National Advisory Committee for Aeronautics,
Langley Field, Va., April 4, 1940.

REFERENCES

1. Wenzinger, Carl J.: Pressure Distribution over an Airfoil Section with a Flap and Tab. T.R. No. 574, N.A.C.A., 1936.

2. Harris, Thomas A.: Reduction of Hinge Moments of Airplane Control Surfaces by Tabs. T.R. No. 528, N.A.C.A., 1935.

3. Goett, Harry J., and Reeder, J. P.: Effects of Elevator Nose Shape, Gap, Balance, and Tabs on the Aerodynamic Characteristics of a Horizontal Tail Surface. T.R. No. 675, N.A.C.A., 1939.

4. Street, William G., and Ames, Milton B., Jr.: Pressure-Distribution Investigation of an N.A.C.A. 0009 Airfoil with a 50-Percent-Chord Plain Flap and Three Tabs. T.N. No. 734, N.A.C.A., 1939.

5. Ames, Milton B., Jr., and Sears, Richard I.: Pressure-Distribution Investigation of an N.A.C.A. 0009 Airfoil with a 30-Percent-Chord Plain Flap and Three Tabs. T.N. No. 759, N.A.C.A., 1940.

6. Wenzinger, Carl J., and Harris, Thomas A.: The Vertical Wind Tunnel of the National Advisory Committee for Aeronautics. T.R. No. 387, N.A.C.A., 1931.

7. Goett, Harry J., and Bullivant, W. Kenneth: Tests of N.A.C.A. 0009, 0012, and 0018 Airfoils in the Full-Scale Tunnel. T.R. No. 647, N.A.C.A., 1938.

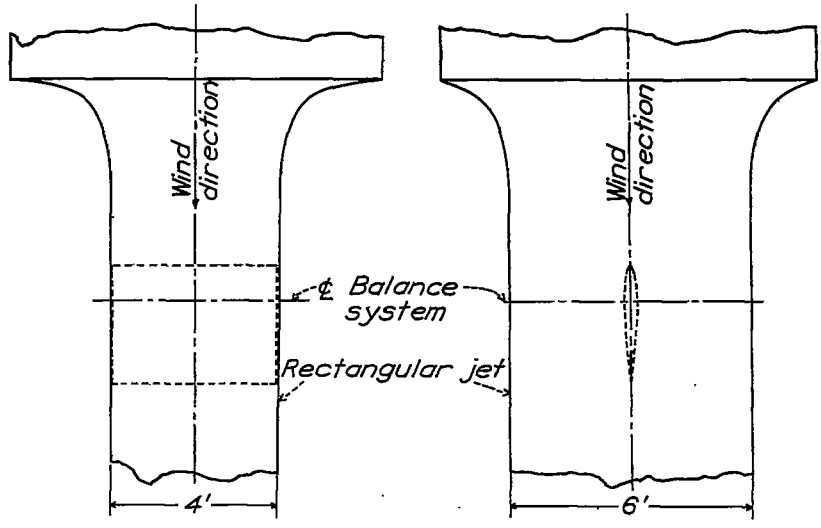

Figure 1.- Model mounted in 4-by 6-foot vertical tunnel.

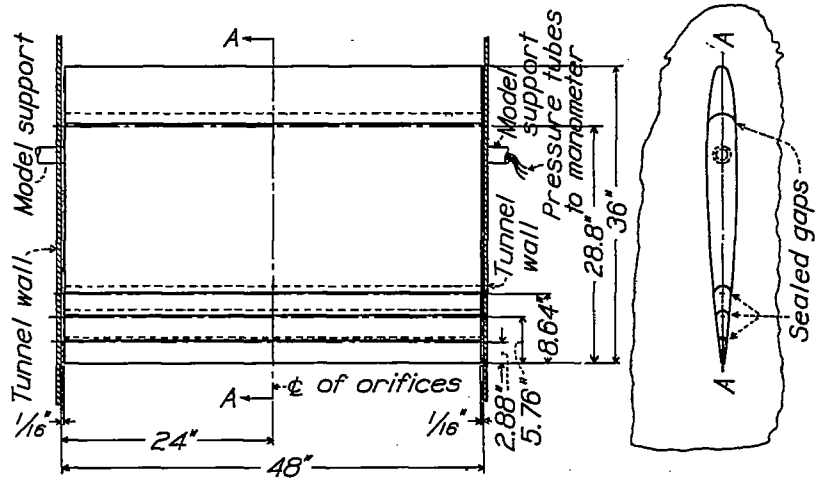

Figure 2.- The N.A.C.A. 0009 pressure-distribution model with 0.80c plain flap and 0.10c_f, 0.20c_f, and 0.30c_f tabs.

Orifice	Location
0	0
1	.62
2	1.25
3	2.5
4	5.0
5	10.0
6	15.0
7	18.0
8	20.0
9	22.5
10	25.0
11	30.0
12	40.0
13	50.0
14	60.0
15	65.0

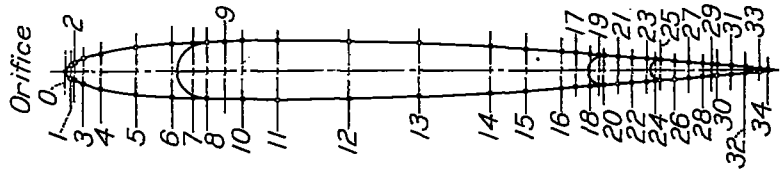

Figure 3.- Chordwise locations of pressure orifices on the N.A.C.A. 0009 airfoil in percent chord.

16	70.0
17	72.0
18	74.0
19	75.25
20	76.0
21	78.0
22	80.0
23	82.0
24	83.25
25	84.0
26	86.0
27	88.0
28	90.0
29	91.25
30	92.0
31	94.0
32	96.0
33	98.0
34	99.25

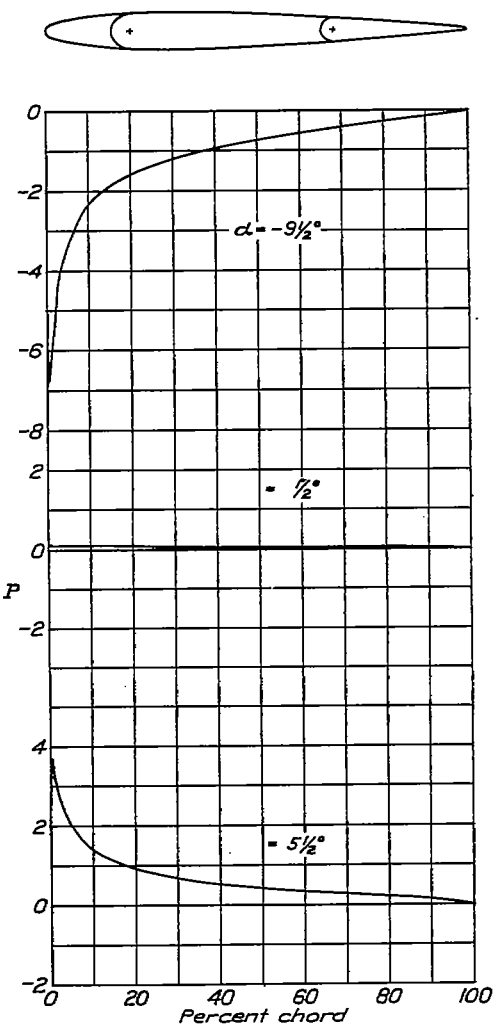

Figure 4.- Distribution of resultant pressure over the N.A.C.A. 0009 airfoil at various angles of attack. Flap and tab neutral.

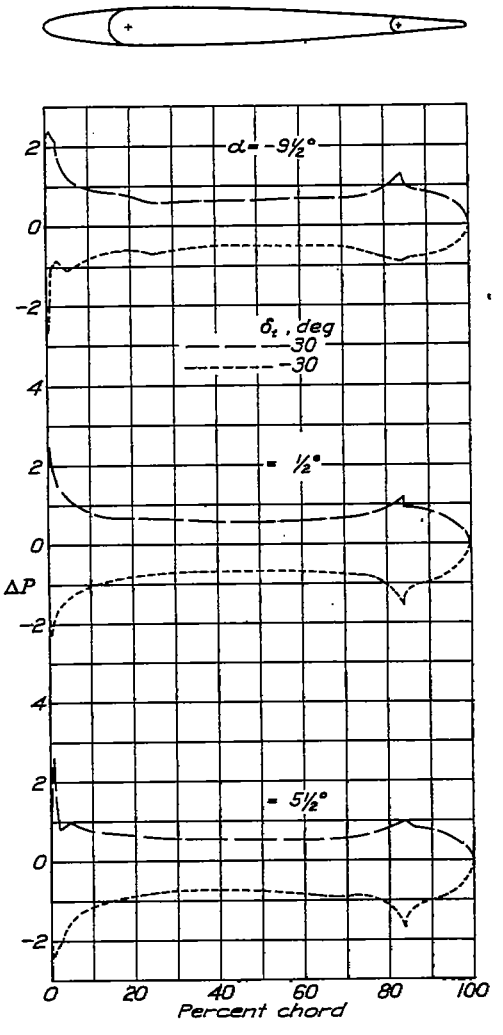

Figure 5.- Increments of resultant pressures for various angles of attack and various deflections of a $0.20c_f$ tab on a 0.80c plain flap deflected 0°.

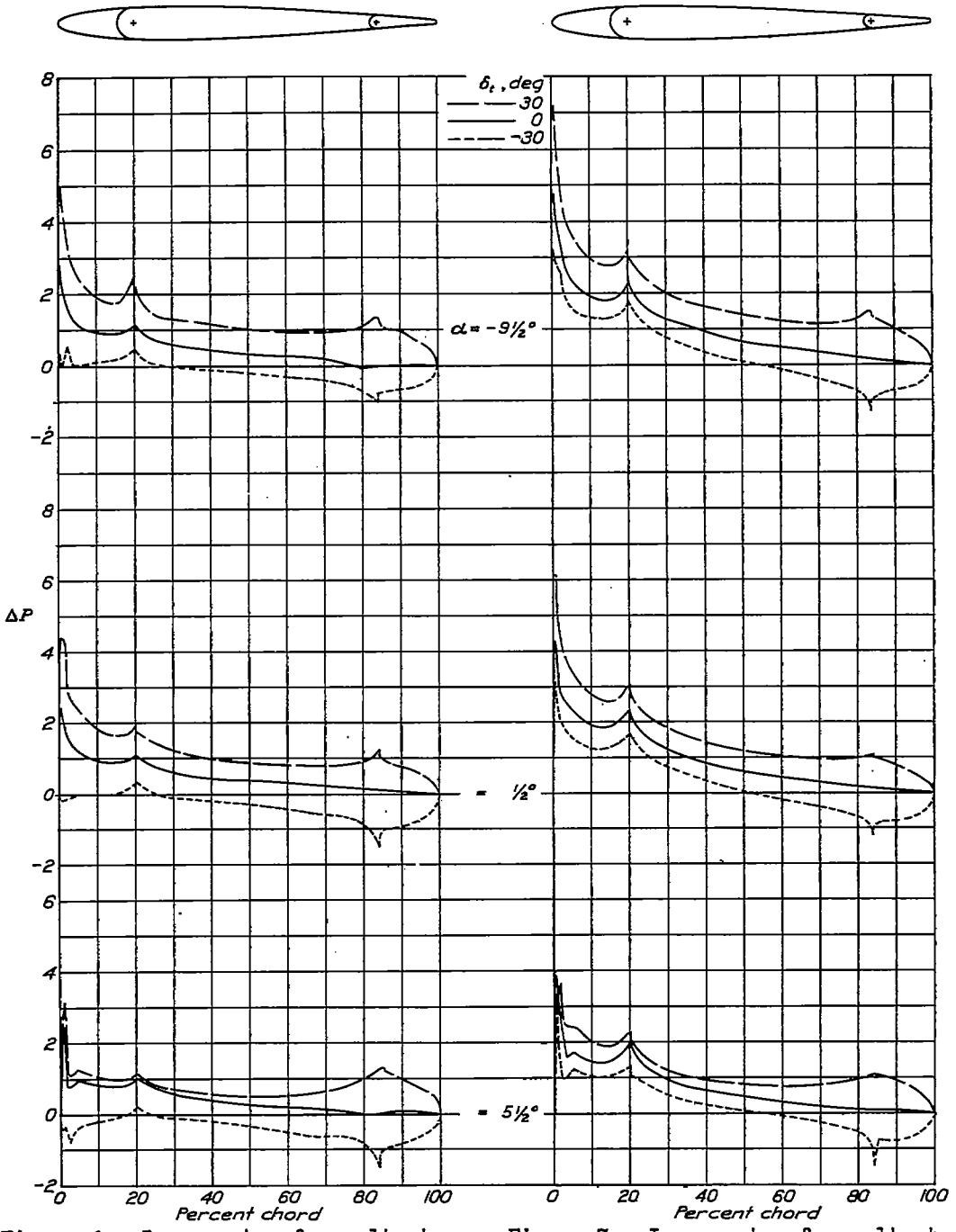

Figure 6.- Increments of resultant pressures for various angles of attack and various deflections of a 0.20c_f tab on a 0.80c plain flap deflected 5°.

Figure 7.- Increments of resultant pressures for various angles of attack and various deflections of a 0.20c_f tab on a 0.80c plain flap deflected 10°.

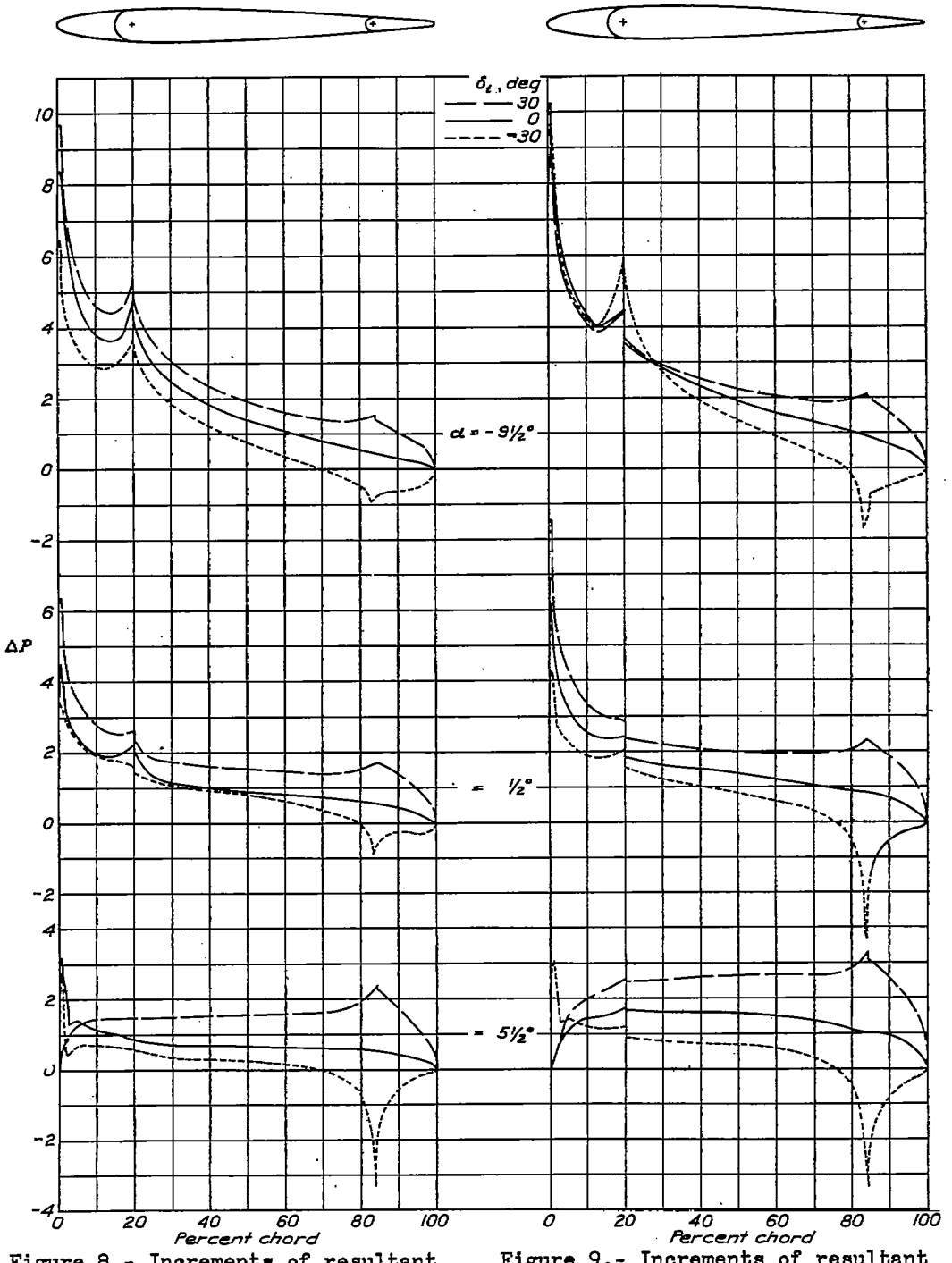

Figure 8.- Increments of resultant pressures for various angles of attack and various deflections of a 0.20c_f tab on a 0.80c plain flap deflected 20°.

Figure 9.- Increments of resultant pressures for various angles of attack and various deflections of a 0.20c_f tab on a 0.80c plain flap deflected 30°.

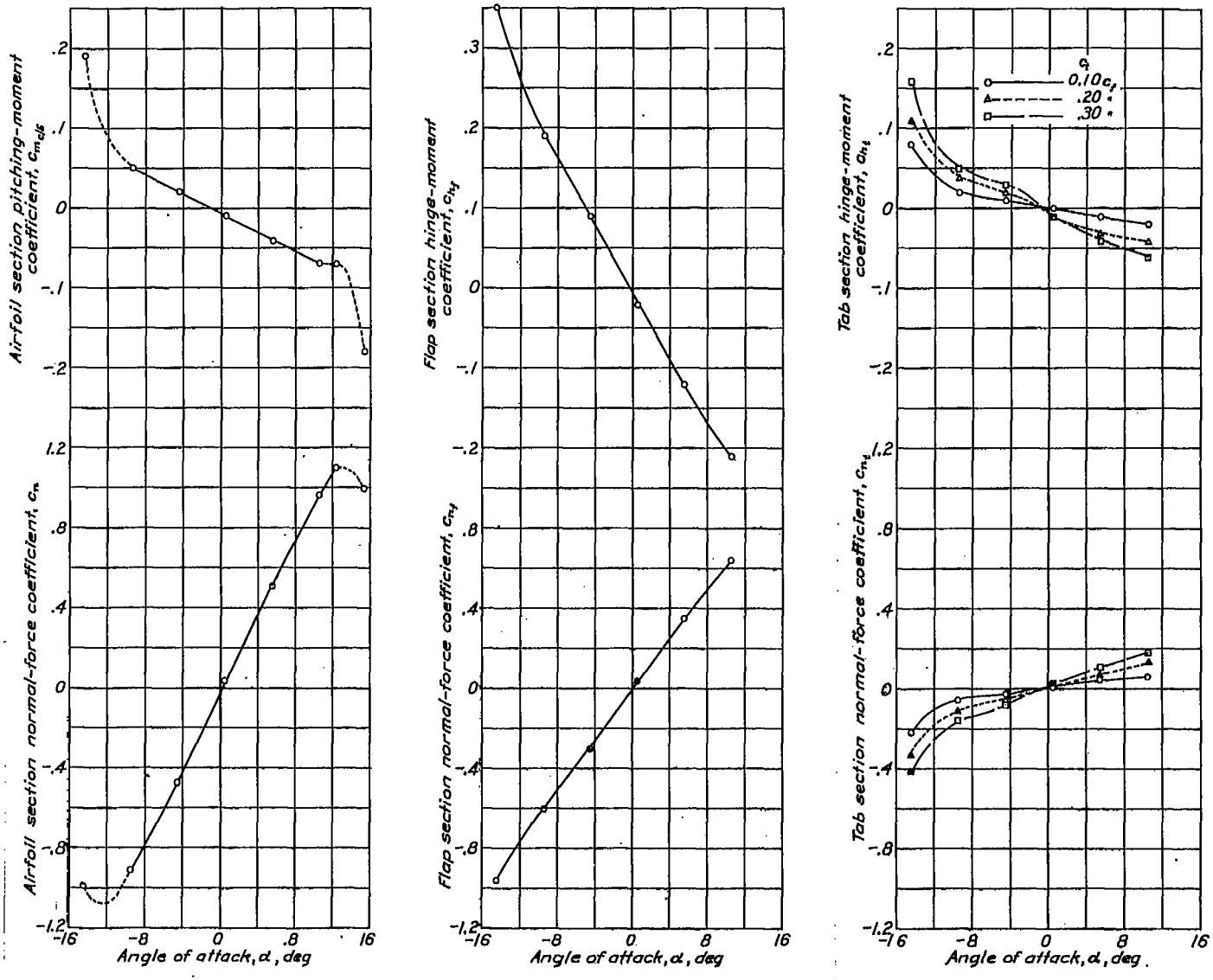

Figure 10.- Section characteristics of basic N.A.C.A. 0009 airfoil with 0.80c plain flap and tabs neutral.

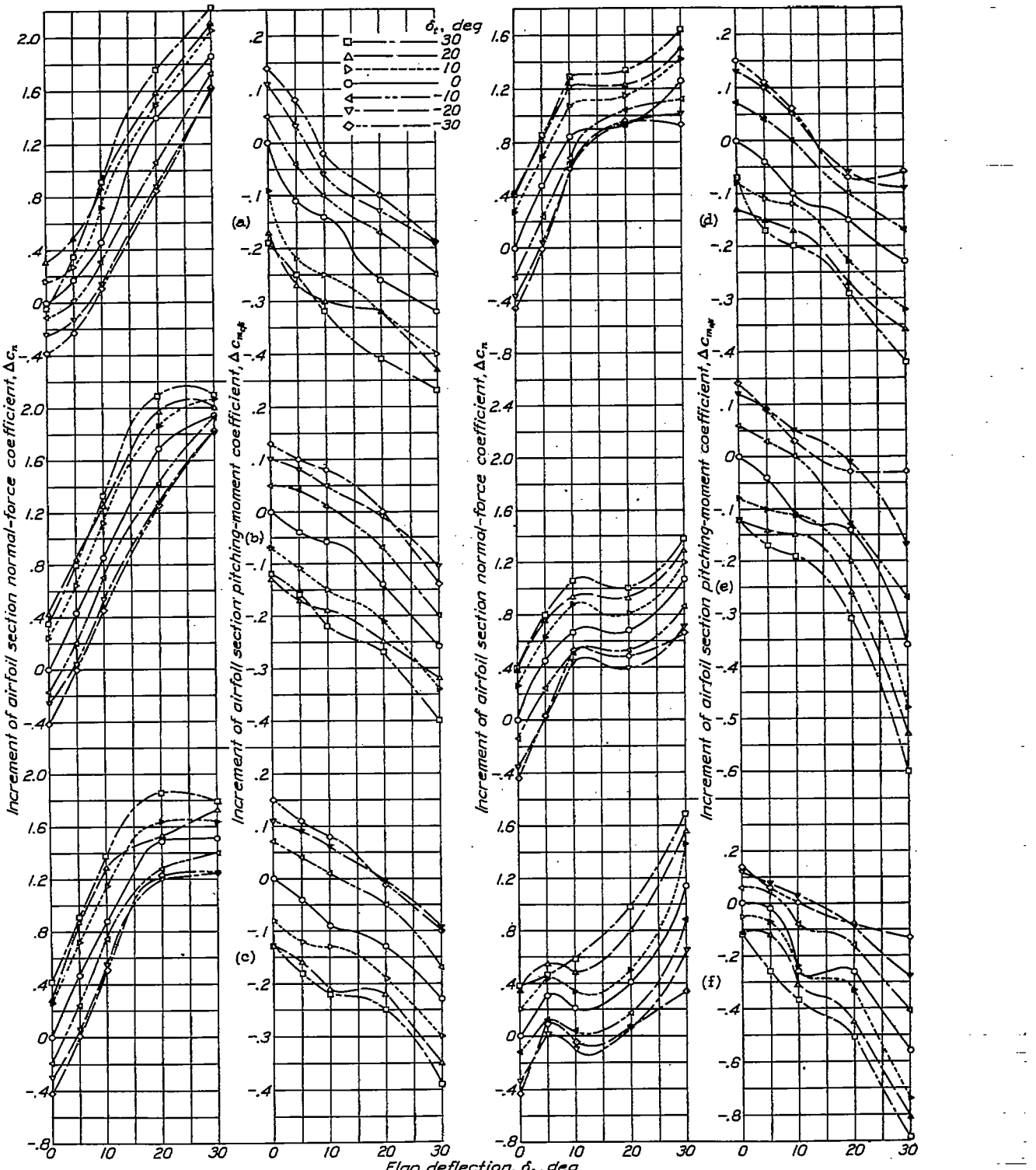

(a) α = -14 1/2° (b) α = -9 1/2° (c) α = -4 1/2° (d) α = 1/2° (e) α = 5 1/2° (f) α = 10 1/2°

Figure 11, a to f.- Increments of airfoil section normal-force and pitching-moment coefficients for various deflections of an 0.80c plain flap and a 0.10c_f tab.

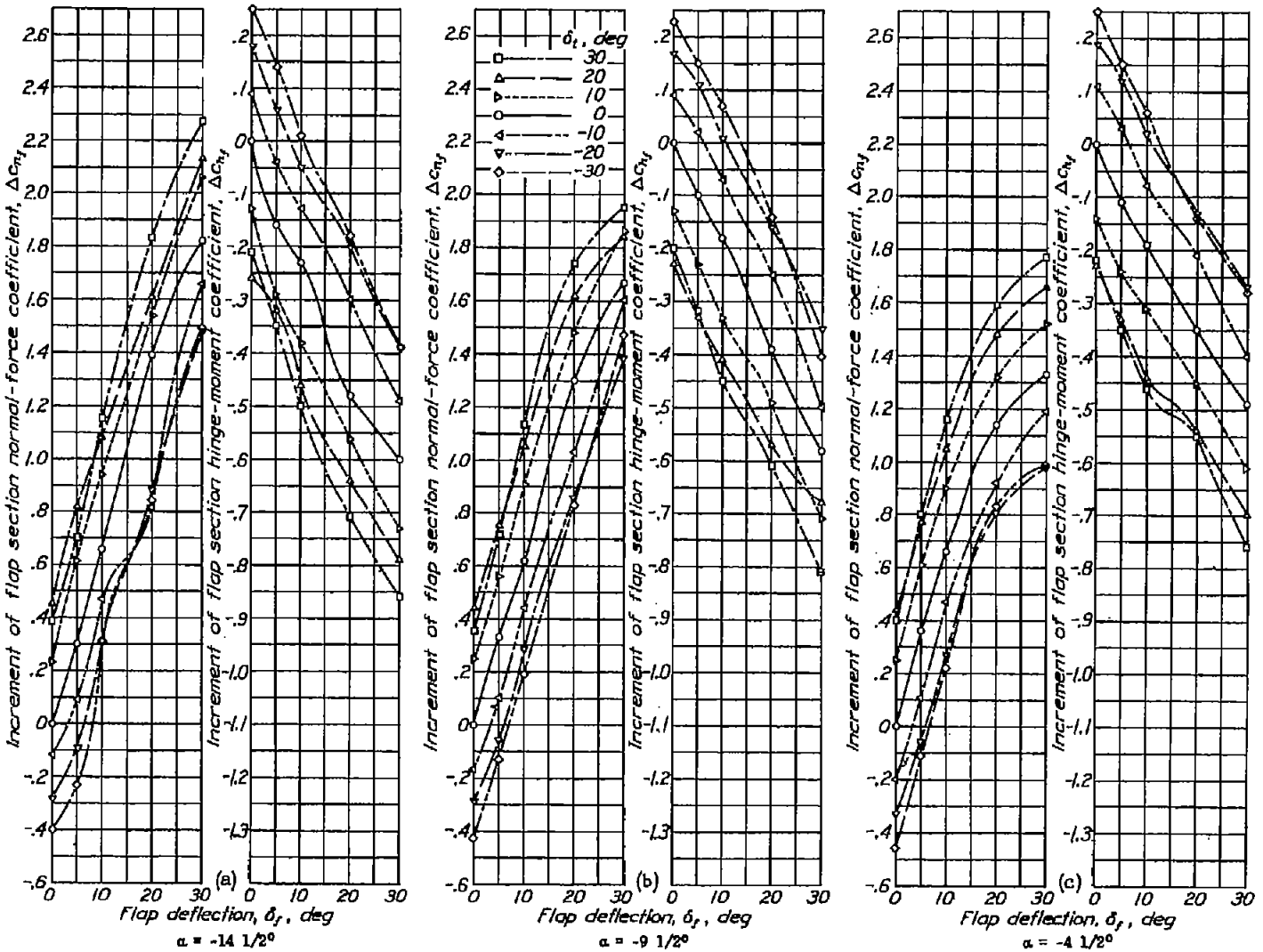

Figure 12, a to f.- Increments of flap section normal-force and hinge-moment coefficients for various deflections of a 0.80c plain flap and a $0.10c_f$ tab.

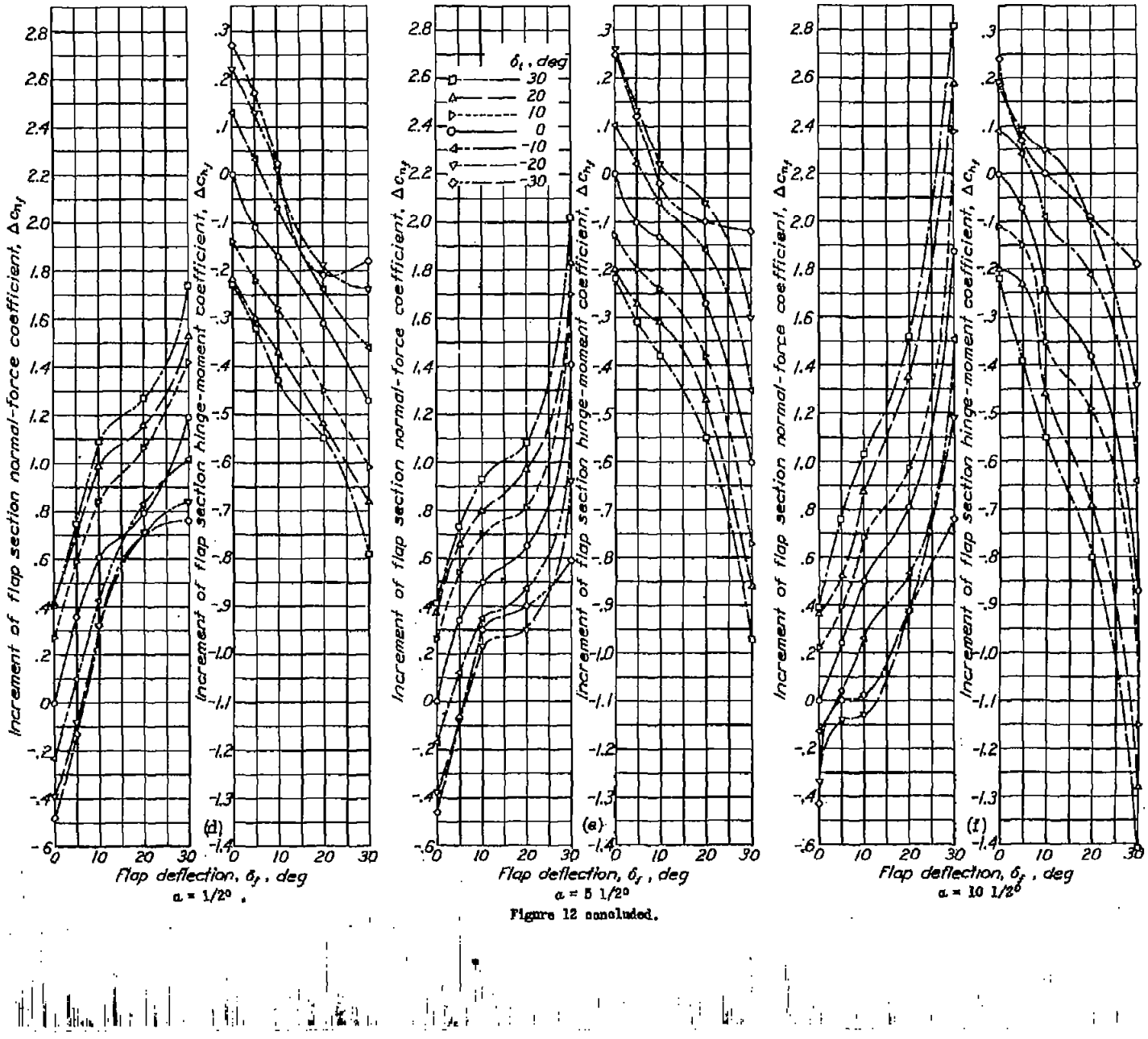

Figure 12 concluded.

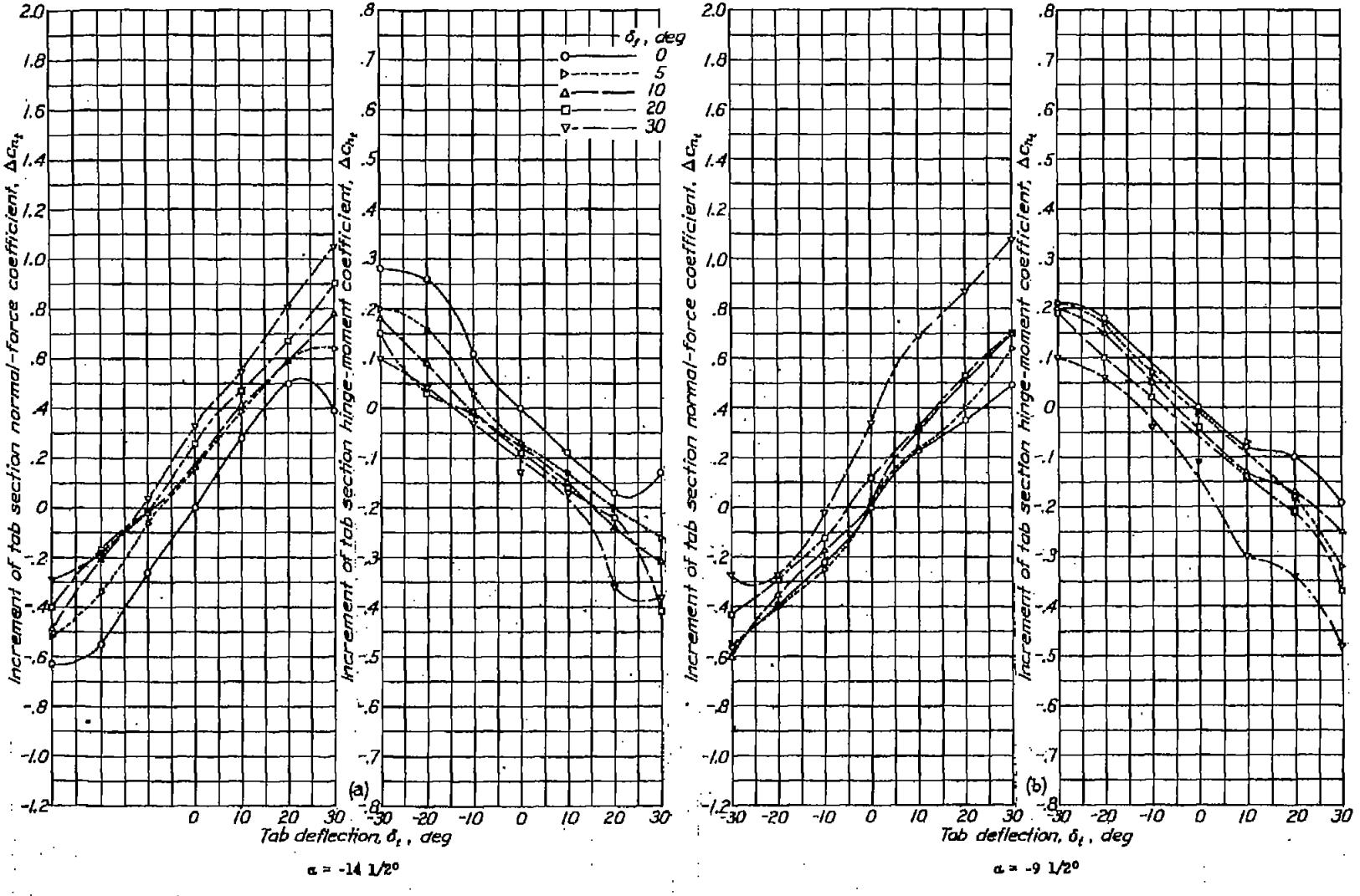

Figure 13,a to f.- Increments of tab section normal-force and hinge-moment coefficients for various deflections of an 0.80c plain flap and a $0.10c_f$ tab.

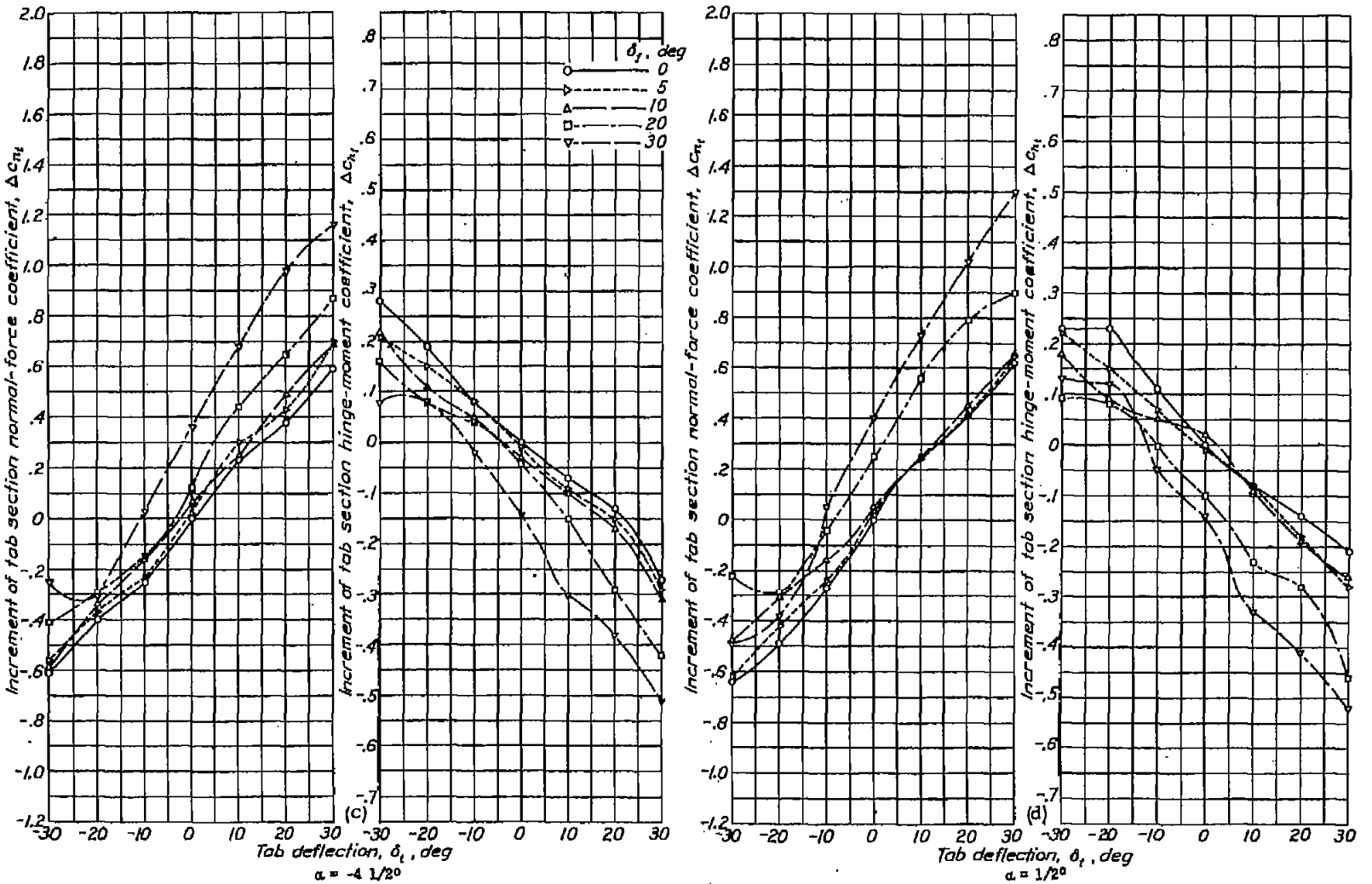

Figure 13 continued.

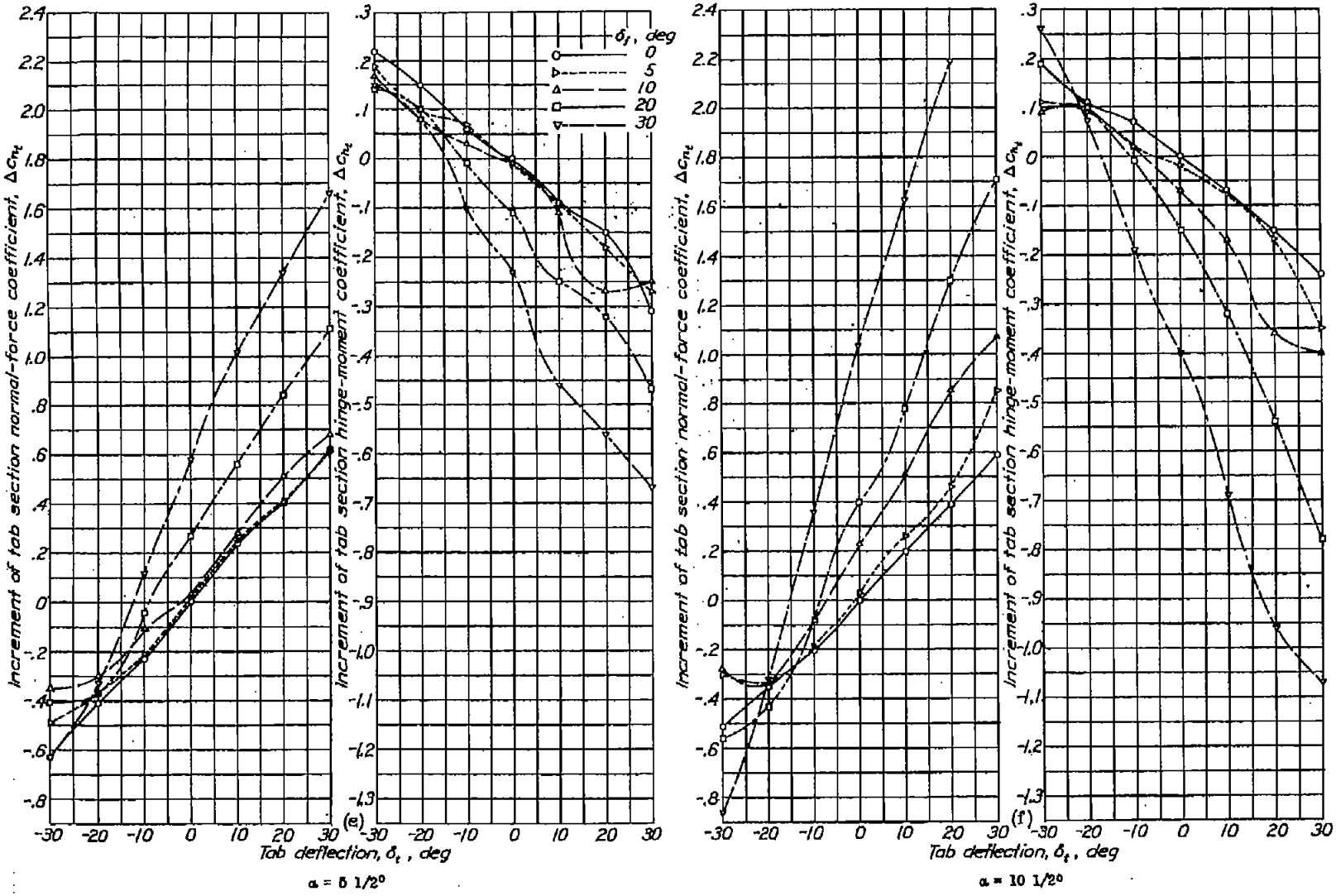

Figure 15 concluded.

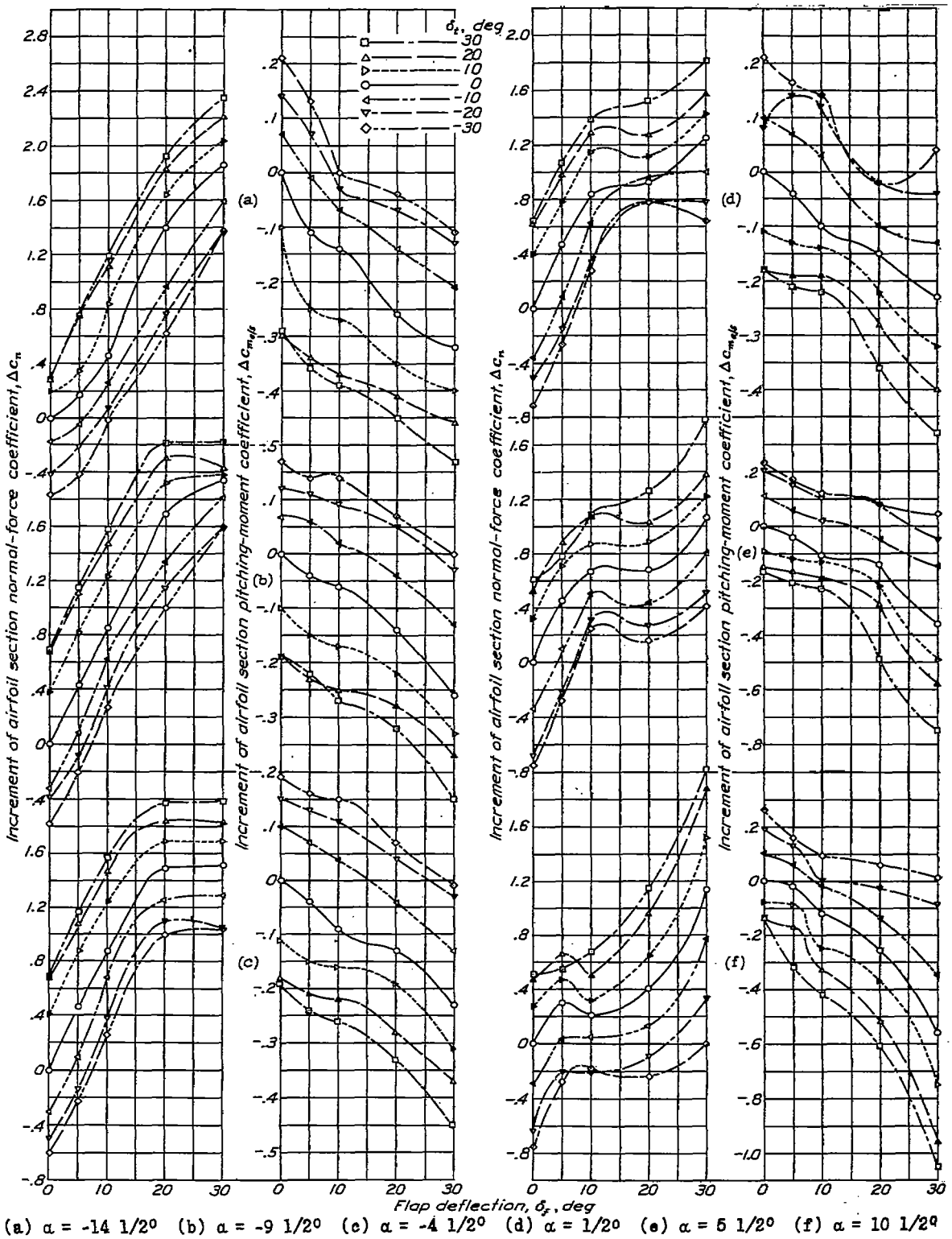

(a) α = -14 1/2° (b) α = -9 1/2° (c) α = -4 1/2° (d) α = 1/2° (e) α = 5 1/2° (f) α = 10 1/2°

Figure 14, a to f.- Increments of airfoil section normal-force and pitching-moment coefficients for various deflections of an 0.80c plain flap and a 0.20c_f tab.

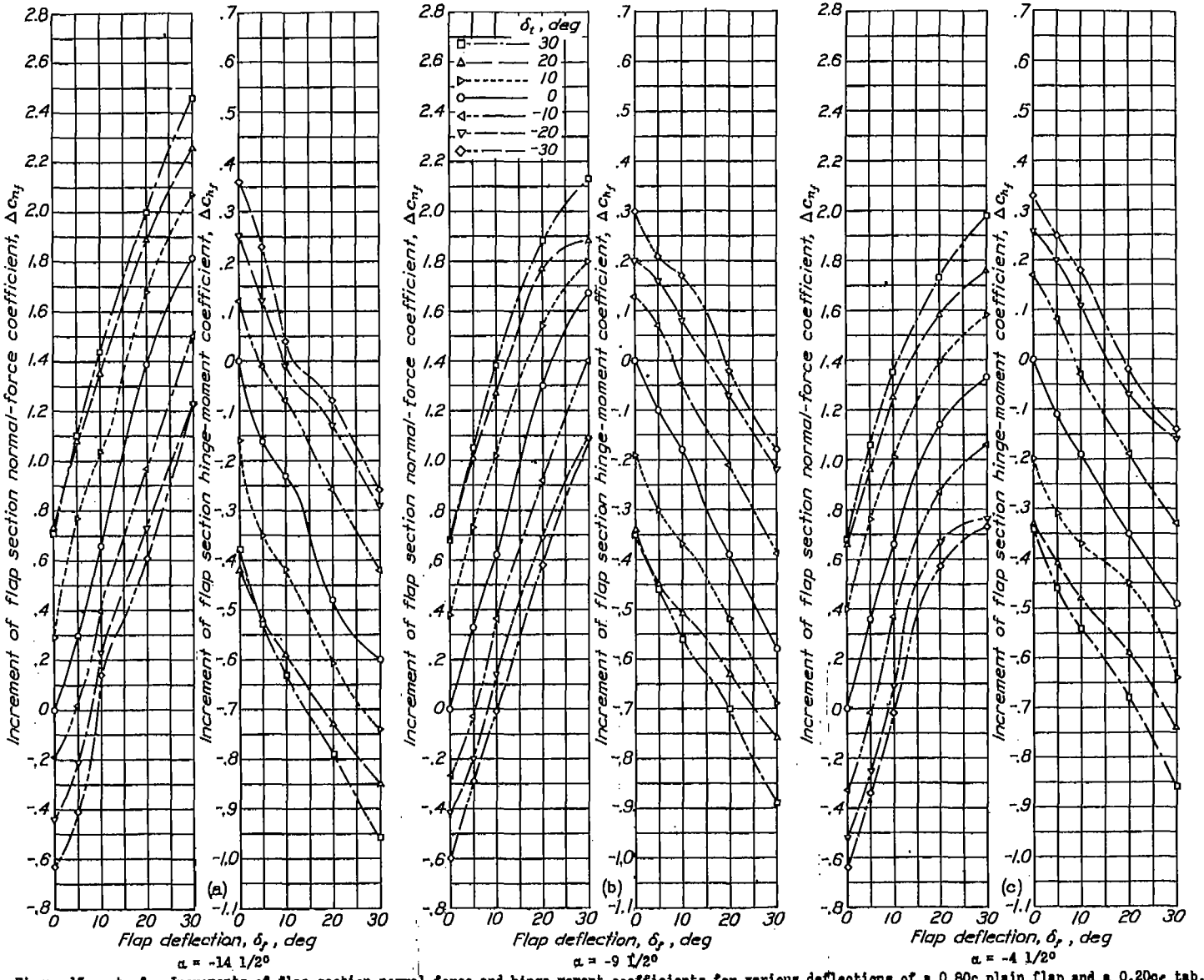

Figure 15, a to f.- Increments of flap section normal-force and hinge-moment coefficients for various deflections of a 0.80c plain flap and a 0.20c_f tab.

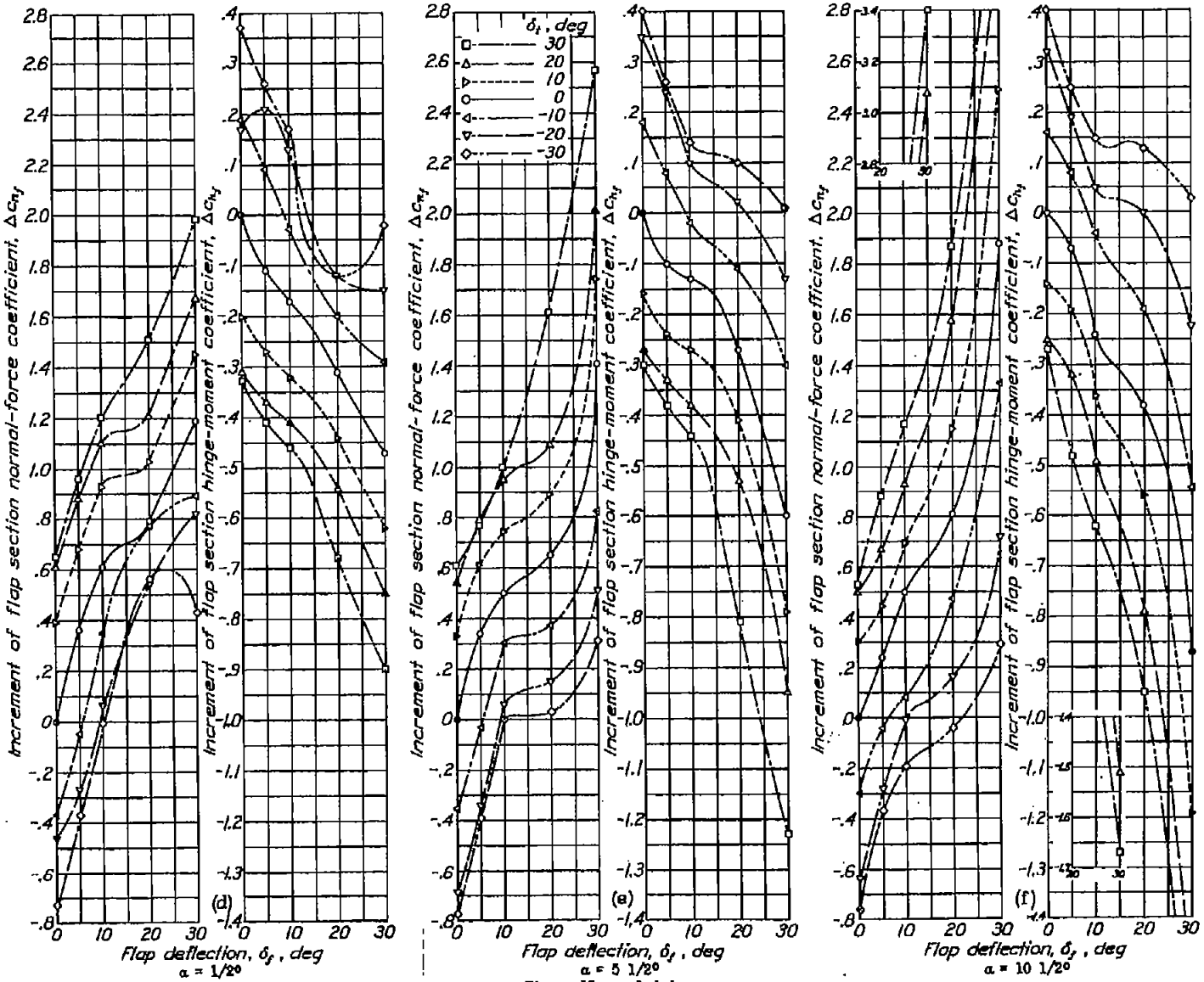

Figure 15 concluded.

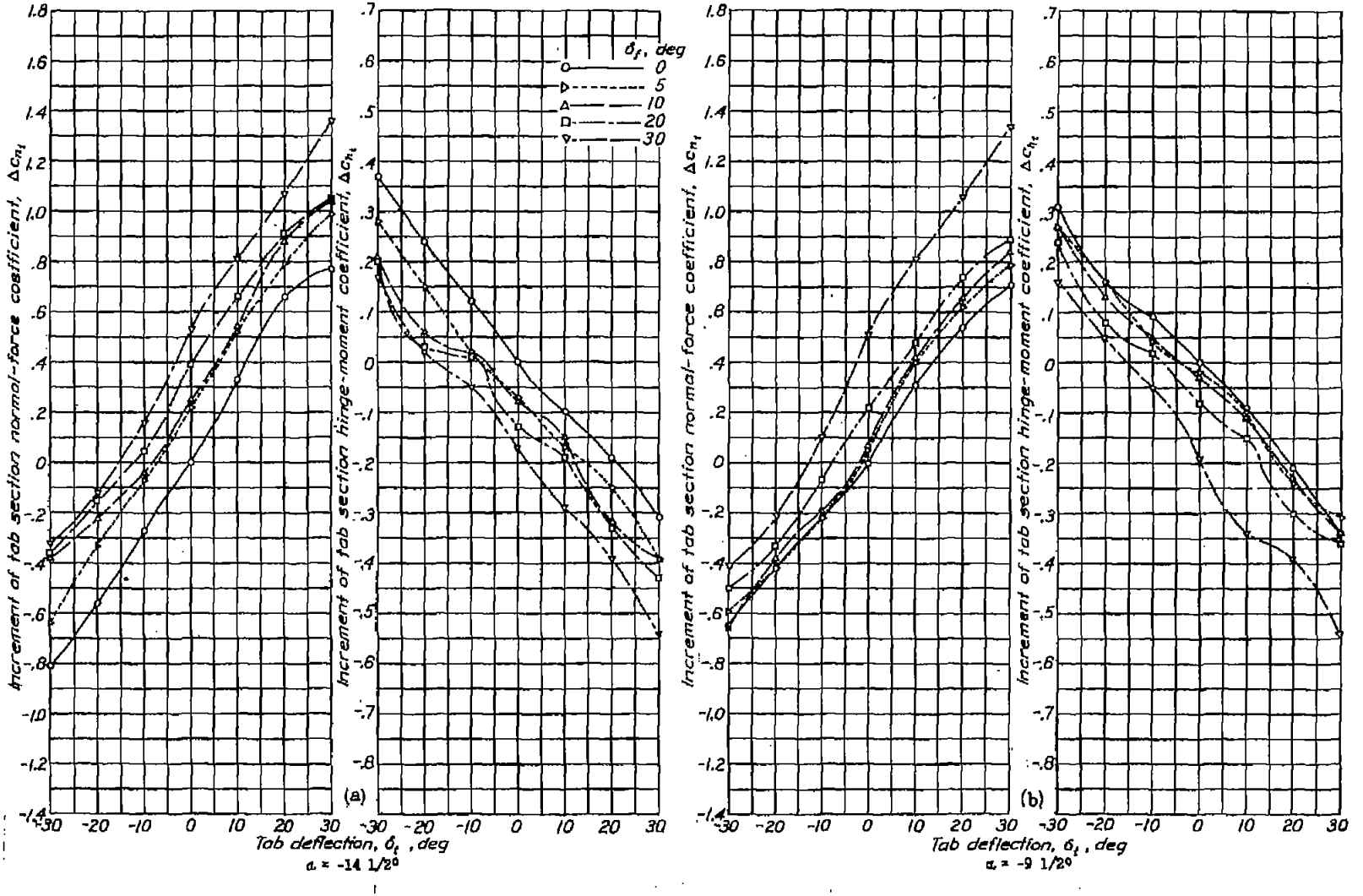

Figure 16, a to f.- Increments of tab section normal-force and hinge-moment coefficients for various deflections of a 0.80c plain flap and a 0.20c$_f$ tab.

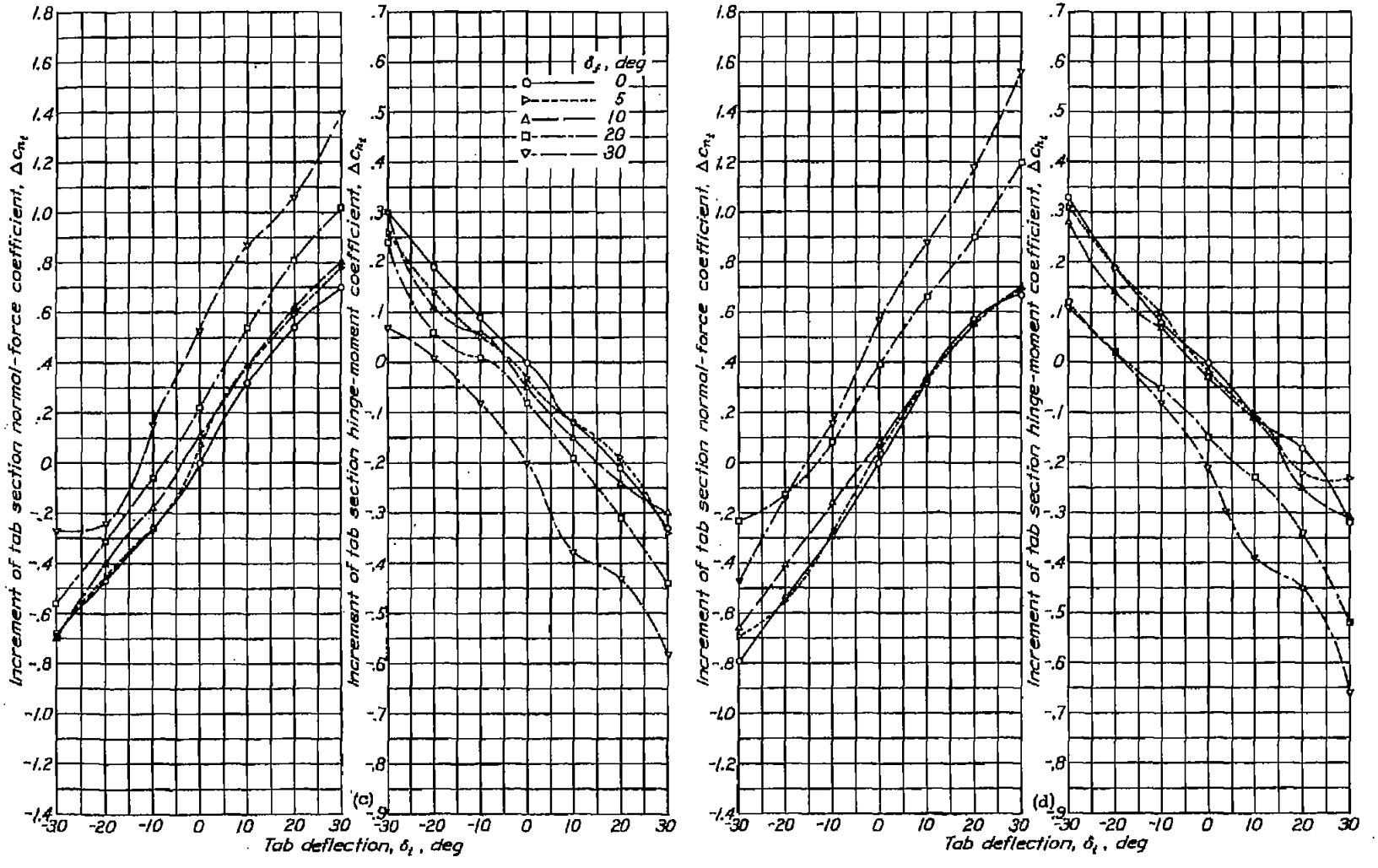

Figure 16 continued.

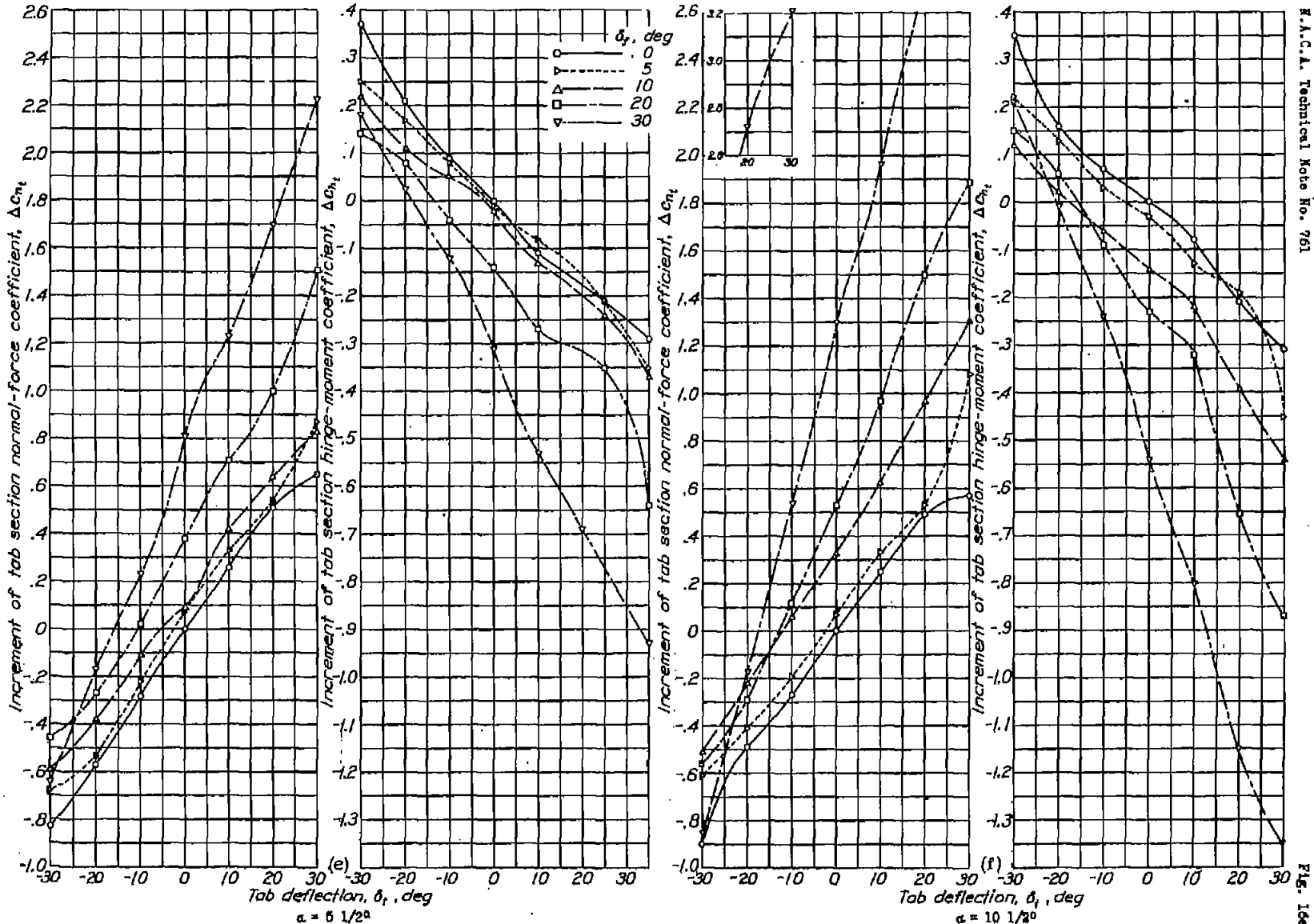

Figure 16 concluded.

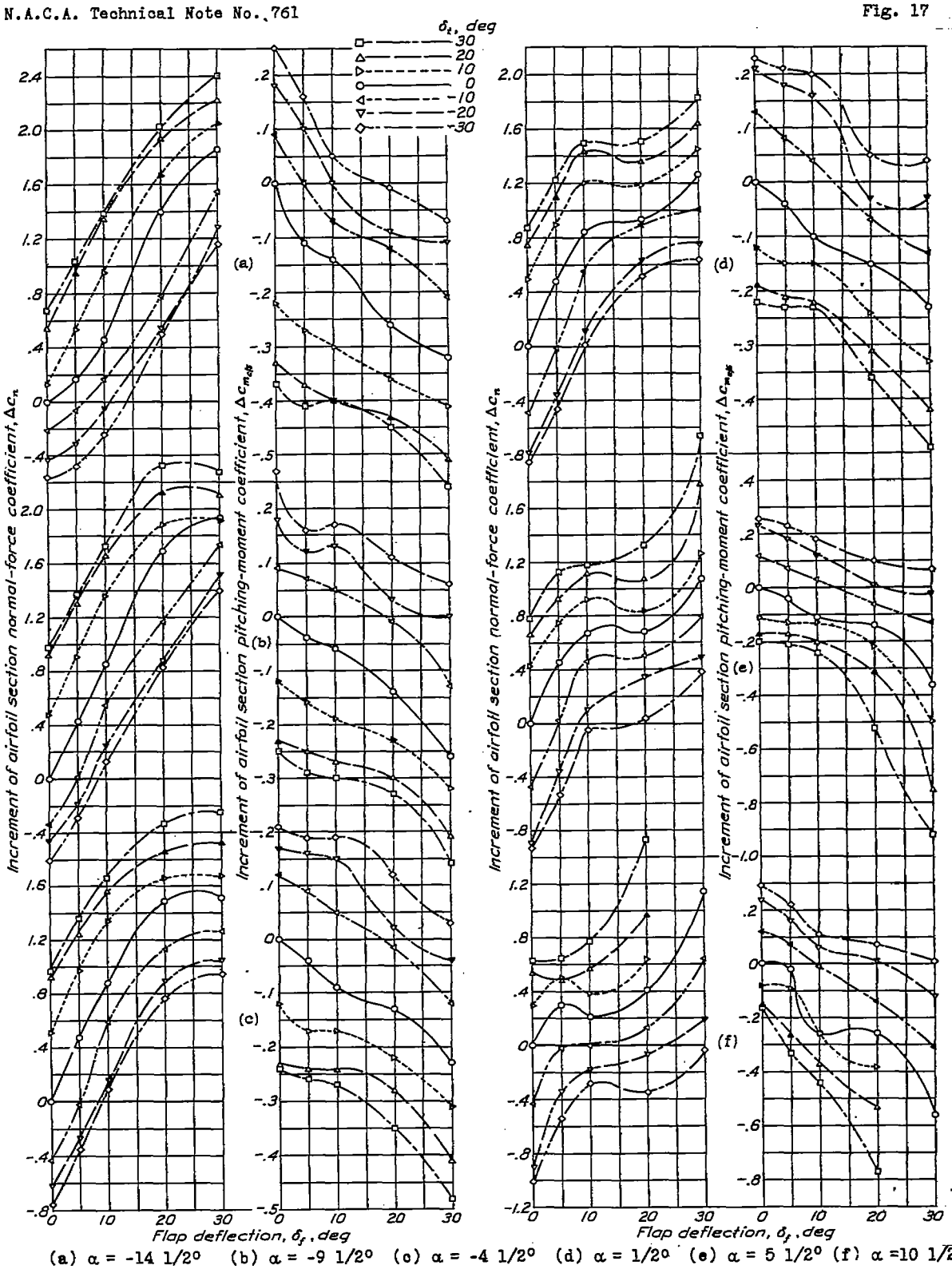

(a) α = -14 1/2° (b) α = -9 1/2° (c) α = -4 1/2° (d) α = 1/2° (e) α = 5 1/2° (f) α =10 1/2°

Figure 17, a to f.- Increments of airfoil section normal-force and pitching-moment coefficients for various deflections of an 0.80c plain flap and a 0.30c_f tab.

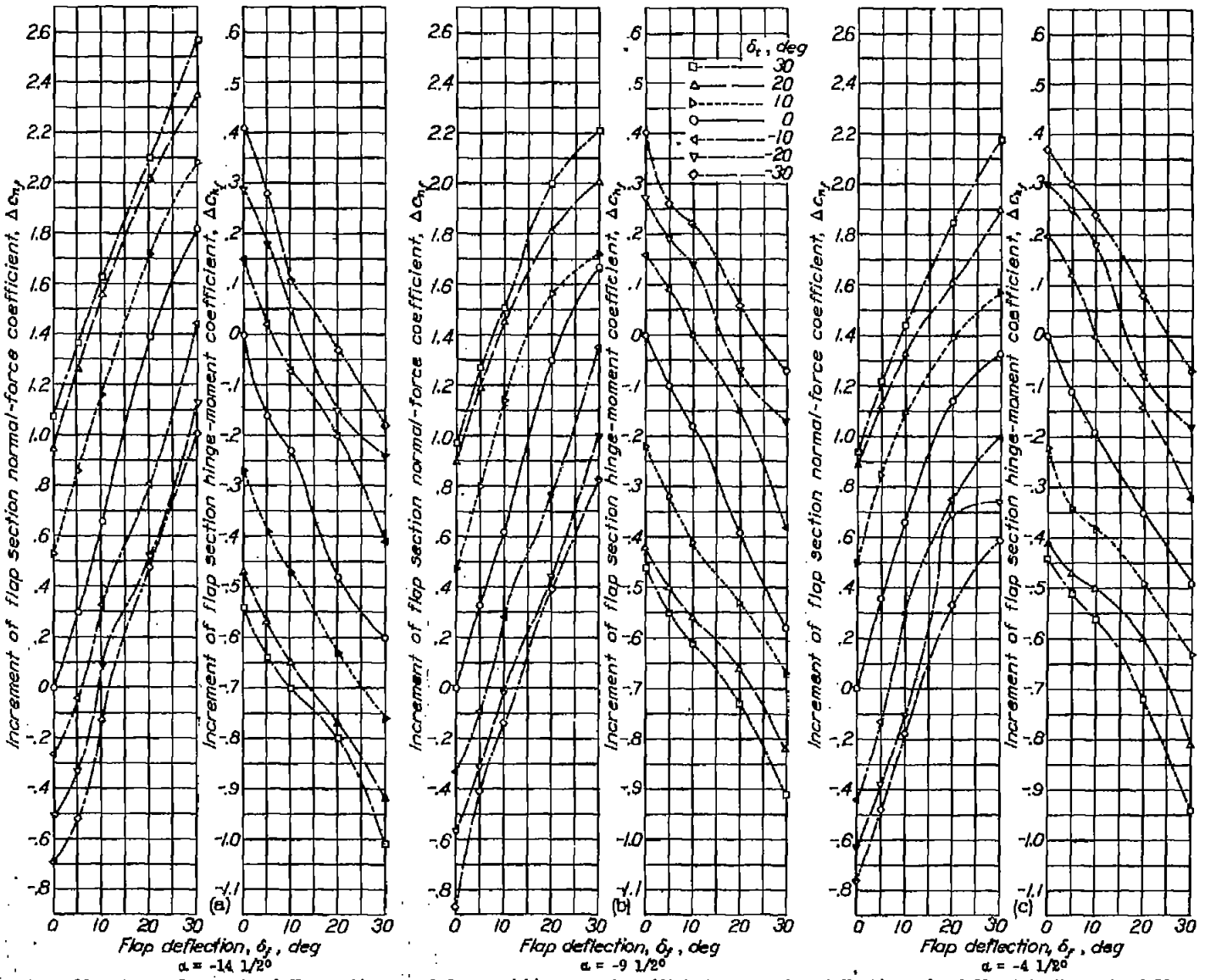

Figure 18, a to f.- Increments of flap section normal-force and hinge-moment coefficients for various deflections of a 0.80c plain flap and a 0.30c$_f$ tab.

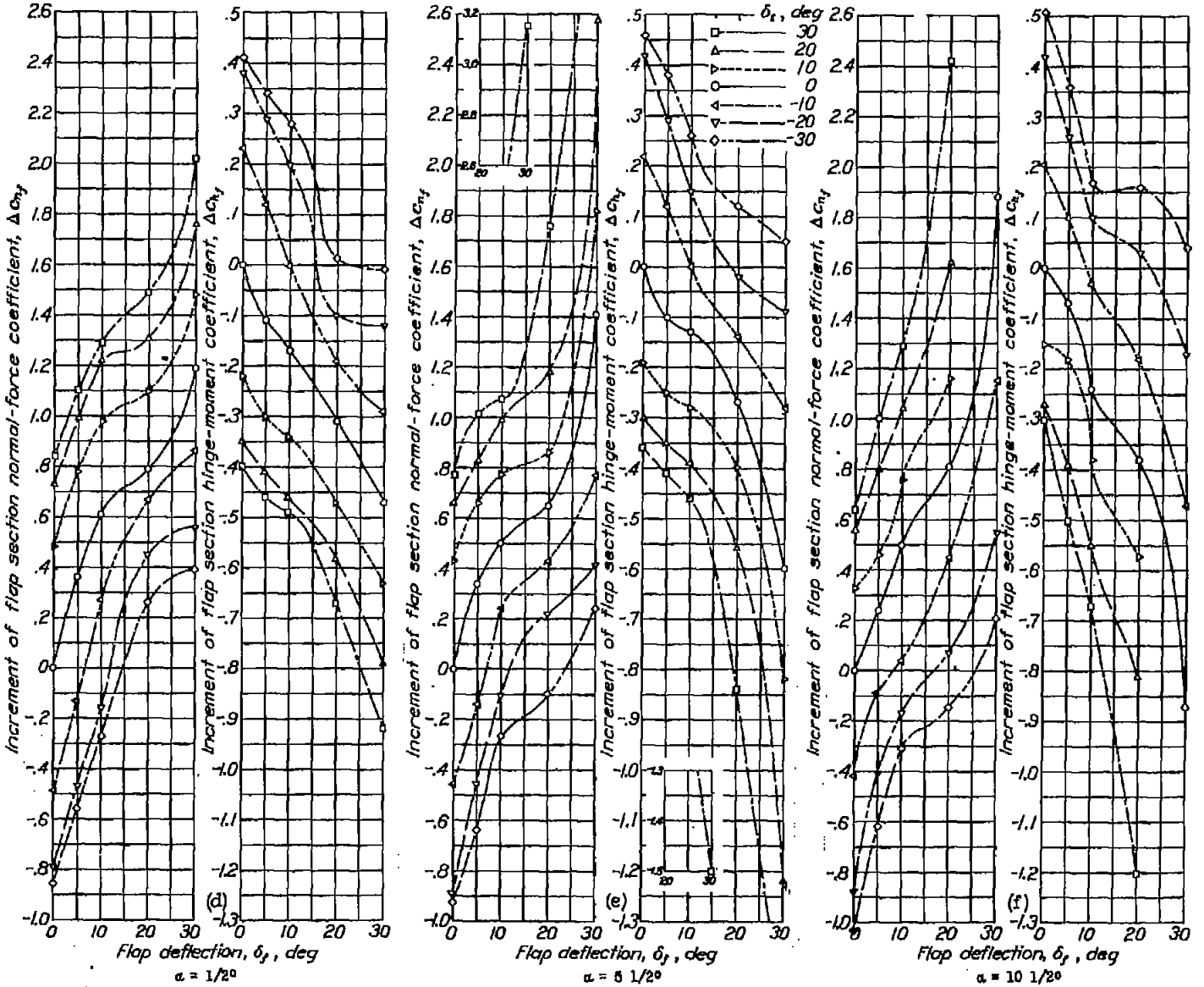

α = 1/2° α = 5 1/2° α = 10 1/2°

Figure 18 concluded.

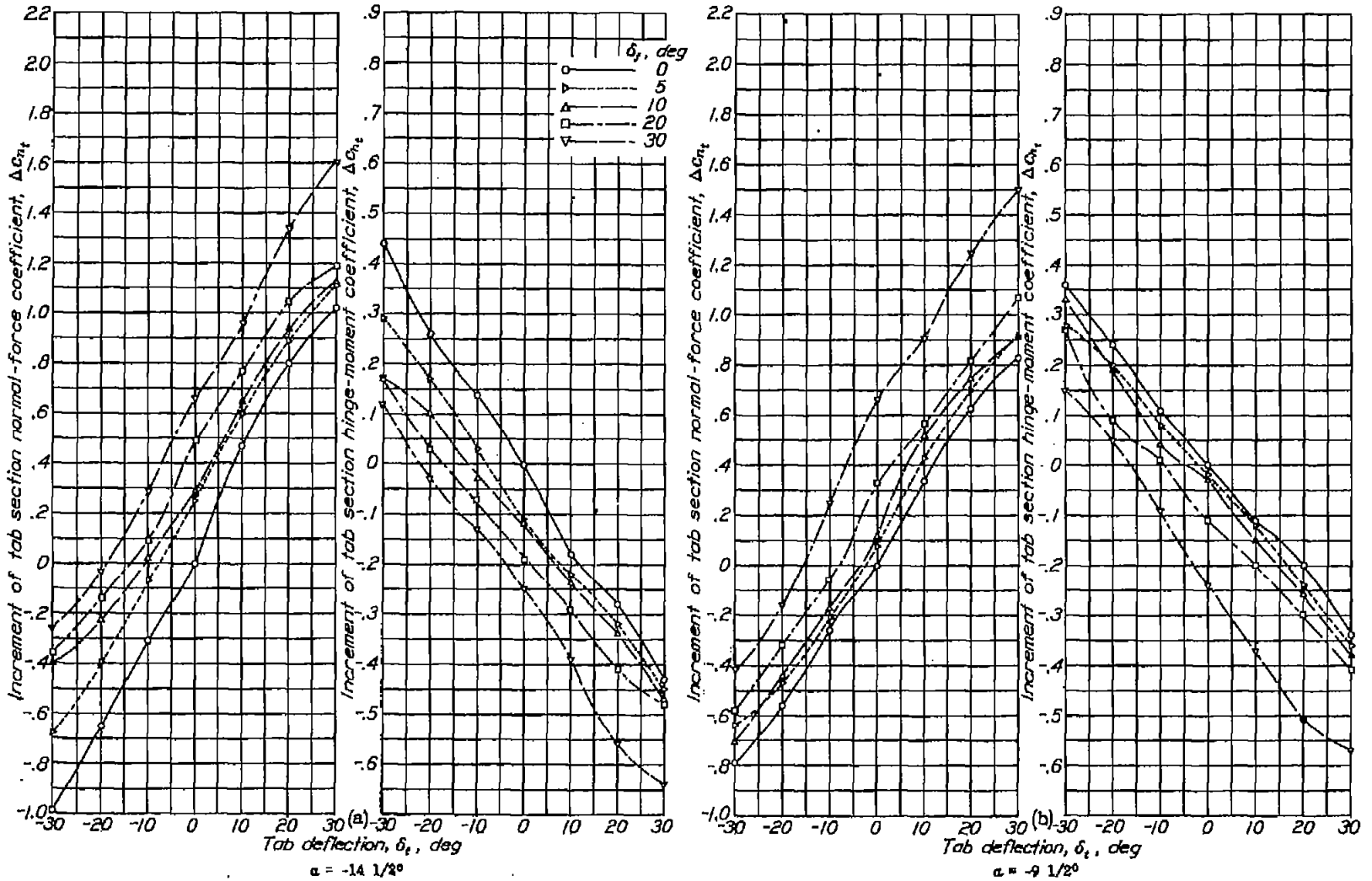

Figure 19, a to f.- Increments of tab section normal-force and hinge-moment coefficients for various deflections of a 0.80c plain flap and a 0.30c$_f$ tab.

Fig. 19a,b

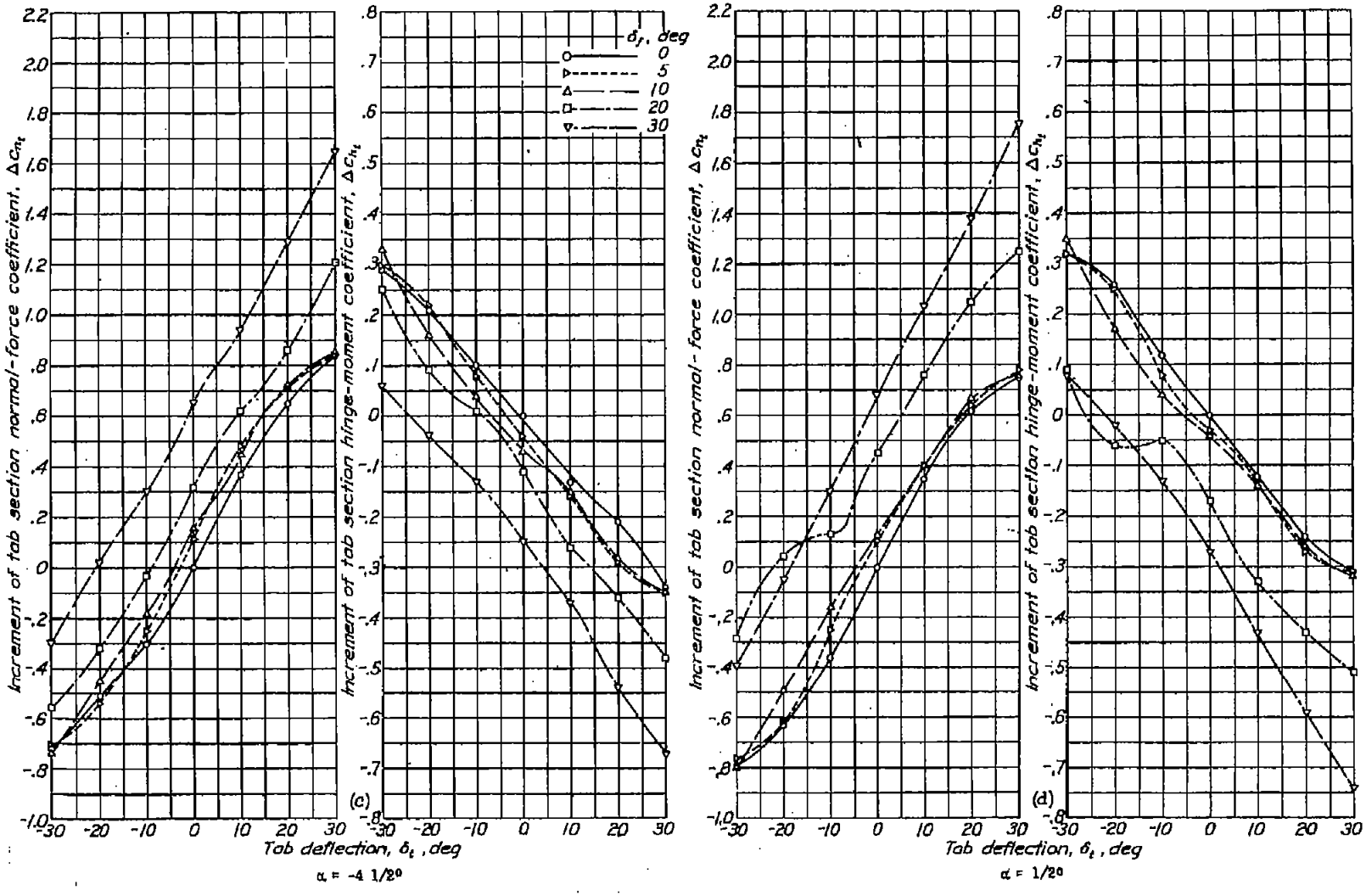

Figure 19 continued.

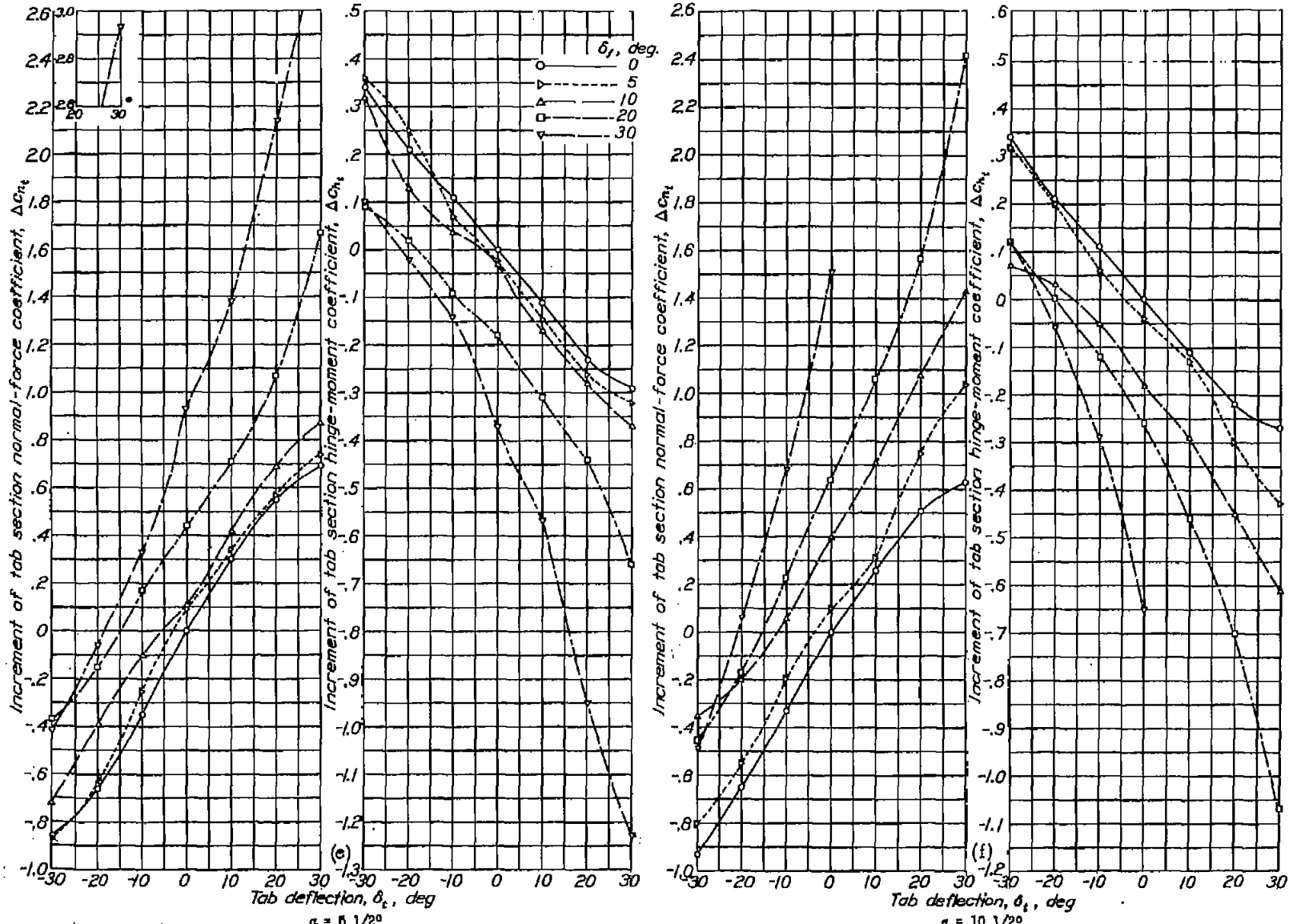

Figure 19 concluded.